Archives of Gynecology and Obstetrics (2019) 299:1715–1725
https://doi.org/10.1007/s00404-019-05122-y

Novel circular RNA expression in the cumulus cells of patients with polycystic ovary syndrome

Zhi Ma[1] · Huishan Zhao[2] · Yan Zhang[3] · Xiaoyan Liu[2] · Cuifang Hao[2]

Received: 14 August 2018 / Accepted: 16 March 2019 / Published online: 2 April 2019

Abstract

Purpose Circular RNAs (circRNAs) mediate the posttranscriptional regulation of multiple genes by functioning as microRNA (miRNA) sponges. This study aimed to detect the novel expression of circRNAs in the cumulus cells (CCs) of polycystic ovary syndrome (PCOS) patients and their potential significance in the pathogenesis of PCOS.

Methods circRNAs in the CCs from 6 PCOS patients and 6 normal control individuals were collected for microarray analysis, and an independent cohort study including 25 PCOS patients and 25 normal control individuals was conducted to validate the circRNA microarray results using quantitative real-time polymerase chain reaction (qRT-PCR). Spearman's rank correlation and receiver operating characteristic (ROC) were performed to delineate the potential correlation between novel circRNAs and patients' clinical characteristics and their potential efficacy for the diagnosis of PCOS. Bioinformatics analysis was applied to investigate the potential roles of circRNAs in the pathogenesis of PCOS.

Results A total of 286 circRNAs (167 upregulated and 119 downregulated) were identified by microarray that was differentially expressed between the PCOS and non-PCOS groups. After qRT-PCR validation, the expression levels of hsa_circ_0043533 ($p < 0.05$) and hsa_circ_0043532 ($p < 0.01$) were significantly higher in the PCOS group, while the expression level of hsa_circ_0097636 ($p < 0.01$) was prominently lower versus the non-PCOS group. Spearman's rank correlation indicated that the serum testosterone (T) level positively correlated with the expression of hsa_circ_0043533 and hsa_circ_0097636 in the PCOS group. The ROC curve analysis found that the combination of hsa_circ_0097636 and T resulted in a larger area under the curve (AUC) (0.893) compared with each circRNA alone (0.709, 0.738, and 0.718 for hsa_circ_0043533, hsa_circ_0097636 and hsa_circ_0043532, respectively). Bioinformatics analysis revealed that the dysregulated circRNAs were potentially involved in cell cycle, oocyte meiosis, progesterone-mediated oocyte maturation, the FOXO signaling pathway, phosphatidylinositol signaling and glycerophospholipid metabolism.

Conclusions The expression of circRNAs in CCs was significantly different between PCOS and normal control individuals. We validated three circRNAs, which could lead to a better understanding of disease pathogenesis and the development of effective therapeutic interventions for PCOS patients.

Keywords Polycystic ovary syndrome · Cumulus cells · Circular RNA · MicroRNA sponge · Posttranscriptional regulation

Introduction

Polycystic ovary syndrome (PCOS) is the most common and heterogeneous endocrine disorder in women of reproductive age. Depending on different criteria and populations, the prevalence of PCOS ranges from 6 to 8% with the NIH criteria, and up to 20% with the Rotterdam criteria [1, 2]. Further, it accounts for approximately 75% of anovulatory infertility [3]. Women with PCOS suffer multiple short-term and long-term complications, including reproductive (hirsutism, amenorrhea, anovulation, infertility, and pregnancy complications), metabolic (dyslipidemia, type 2 diabetes mellitus,

Electronic supplementary material The online version of this article (https://doi.org/10.1007/s00404-019-05122-y) contains supplementary material, which is available to authorized users.

✉ Cuifang Hao
cuifang-hao@163.com

[1] Medical College of Qingdao University, Qingdao, Shandong, People's Republic of China

[2] Centre for Reproductive Medicine, Yantai Yuhuangding Hospital Affiliated to Qingdao University, Yantai, Shandong, People's Republic of China

[3] Institute of Zoology, Chinese Academy of Sciences, Beijing, People's Republic of China

and cardiovascular risk factors) and psychological (depression, anxiety, body image, and quality of life) disorders [4].

Circular RNAs (circRNAs), a class of noncoding RNAs, were named for their covalently closed loop structures with the absence of a canonical 5′ cap and 3′ poly A tail. Recently, they were found to be stably conserved in diverse types of eukaryotes; they are resistant to RNAse R, and often exhibit spatiotemporal specific expression [5]. By functioning as microRNA (miRNA) sponges, modifiers of alternative splicing and regulators of parental gene expression, circRNAs can regulate the progression of many diseases at the transcriptional and posttranscriptional level [6]. Many studies have revealed the potential close relationship between circRNAs and the initiation and development of many diseases and physiological processes, especially in tumors [7–10]. More recently, circRNA expression profiling of preimplantation embryos and human granulosa cells during maternal aging was investigated, showing a promising correlation with the development of oocytes and embryos [11, 12].

The aim of this study was to investigate the circRNA expression profile of CCs isolated from the cumulus–oocyte complex (COC) of PCOS and normal control patients undergoing controlled ovarian stimulation cycles by performing circRNA microarray analysis and to assess their potential significance in the pathogenesis of PCOS, which may serve as novel biomarkers for the accurate diagnosis and effective therapeutic intervention of PCOS.

Materials and methods

Subjects and protocol

Participants were scheduled for in vitro fertilization (IVF) or intracytoplasmic sperm injection (ICSI) at the Center for Reproductive Medicine of Yantai Yuhuangding Hospital affiliated to Qingdao University (Shandong, People's Republic of China) from May to November 2017. To investigate the expression profiles of novel circRNAs, CCs from 6 PCOS and 6 normal control participants were analyzed with microarray. qRT-PCR was conducted in an independent cohort (PCOS group, $n = 25$; control group, $n = 25$) to validate the microarray results. All participants in the PCOS group ($n = 25$) were included under the Rotterdam two of three criteria [13]: oligo-ovulation or anovulation; polycystic ovarian morphology (PCOM) on ultrasonography; and hyperandrogenism with the exclusion of other etiologies such as congenital adrenal hyperplasia, Cushing's syndrome and androgen-secreting tumors. Participants in the non-PCOS group ($n = 25$) were those who sought assisted reproductive techniques primarily due to male factors or problems with fallopian tubes (salpingemphraxis or salpingectomy on both sides); patients with endometriosis, thyroid disease, abnormal endocrine condition and other systematic diseases were all excluded. Basal serum hormone levels including follicular stimulating hormone (FSH), luteinizing hormone (LH), estradiol (E_2), testosterone (T) and progesterone (P) were measured on day 2 of the menstrual cycle before ovarian stimulation. Information regarding anti-Müllerian hormone (AMH), inhibin B (INHB) and 25-(OH)D_3 was also collected. All participants provided written informed consent prior to study commencement.

Each participant in both groups underwent a conventional agonist protocol as previously described by Huang et al. [14]. Briefly, the gonadotropin-releasing hormone agonist (GnRH-a) triptorelin acetate (0.05 mg/day, diphereline; Ipsen Pharma Biotech, France) was applied subcutaneously during the mid-luteal phase. Once pituitary function was fully downregulated, as evidenced by a serum LH level < 3.0 ng/mL and serum E_2 level < 30 pg/mL, the patients would subcutaneously receive recombinant FSH (150–187.5 IU, Puregon, follitropin beta; Merck & Co., Inc. USA) for controlled ovarian stimulation. When two or more follicles were ≥ 18 mm in diameter and the serum E_2 level was greater than 300 pg/mL per dominant follicle, participants were supposed to receive 250 μg hCG (Profasi; Merck Serono, Switzerland) to facilitate ovulation. The clinical characteristics of all participants in the two groups are shown in Table 1.

Cumulus cell isolation

COC retrieval was performed by transvaginal puncture under the guidance of ultrasonography 36 h after hCG administration. CCs surrounding each single oocyte were carefully isolated by mechanical stripping with syringe needles, and CCs from all oocytes per patient were pooled together as one sample. After washing in phosphate-buffered saline (HyClone, GE Healthcare Life Sciences, USA) three times, CCs were then stored at − 80 °C until RNA extraction.

Total RNA extraction and reverse transcription

Total RNA was extracted from cumulus cells using Trizol reagent (Takara, Japan) according to the manufacturer's protocol. OD260/280 readings from a spectrophotometer (NanoDrop ND-1000) were used to determine the purity and concentration of sample RNA. RNA integrity was also determined by 1% formaldehyde denaturing gel electrophoresis. A total of 1000 ng RNA was added to the 20 μl reverse transcription system depending on the concentration of each sample, and random primers were used in the following step according to the recommendations of the QuantiTect Reverse Transcription Kit (QIAGEN GmbH, Hilden, Germany).

Table 1 Comparison of clinical characteristics and hormone levels

Variables	PCOS ($n=25$)	Normal ($n=25$)	p value
Age	29.60 ± 2.76	31.16 ± 3.28	NS
BMI (kg/m^2)	24.46 ± 2.47	21.16 ± 2.04	**< 0.001**
AMH (ng/mL)	12.27 ± 4.88	5.73 ± 2.78	**< 0.001**
LH (mIU/mL)	9.99 ± 5.18	5.56 ± 1.63	**< 0.001**
FSH (mIU/mL)	6.12 ± 1.08	7.09 ± 1.56	**< 0.05**
LH/FSH	1.62 ± 0.77	0.81 ± 0.25	**< 0.001**
E_2 (pg/mL)	34.72 ± 12.26	40.02 ± 23.17	NS
T (ng/mL)	0.40 ± 0.19	0.23 ± 0.12	**< 0.001**
P (ng/mL)	0.83 ± 0.42	0.61 ± 0.26	**< 0.05**
PRL (ng/mL)	17.99 ± 7.63	17.88 ± 1.42	NS
INHB (ng/L)	121.55 ± 55.59	111.11 ± 7.8	NS
25-(OH)D_3 (ng/mL)	21.43 ± 13.96	23.11 ± 2.82	NS
Total Gn dosage (IU)	1697 ± 491.75	1884 ± 538.14	NS
Oocytes obtained	14.52 ± 5.64	10.40 ± 3.41	**< 0.01**
Mature oocytes[a]	12.50 ± 4.44	9.58 ± 3.06	**< 0.05**
Rate of mature oocytes[b]	0.86 ± 0.11	0.91 ± 0.10	NS
HQ embryos[c]	5.92 ± 3.99	4.12 ± 2.88	NS
Rate of HQ embryos[d]	0.59 ± 0.29	0.60 ± 0.33	NS

Data are presented as the mean ± SD, $p < 0.05$ is in bold and considered to be statistically significant

BMI body mass index, *AMH* anti-Müllerian hormone, *LH* luteinizing hormone, *FSH* follicle-stimulating hormone, E_2 estradiol, *T* testosterone, *P* progesterone, *PRL* prolactin, *INHB* inhibin B, *Gn* gonadotropin, *NS* no significant difference, *HQ* high quality

[a]Mature oocytes in our center are defined as those from follicles which contain more than 2 ml of follicle fluid

[b]Mature oocytes rate = number of mature oocytes/oocytes obtained

[c]High-quality embryo in our center is defined as grade 1 or 2 embryo with 6–9 cells on the 3rd day of fertilization

[d]HQ embryos rate = number of HQ embryos /2PN zygotes on the 3rd day

CircRNA microarray and data analysis

Human CircRNA Array v2 (CapitalBio Corporation, Beijing, People's Republic of China) with four identical arrays per slide (4 × 180 K format) was applied to detect circRNAs with differential expression in cumulus cells between PCOS patients and normal controls. Each array contained probes interrogating approximately 170,340 human circRNAs. Those circRNA target sequences are all from Circbase, Deepbase and Rybak-Wolf2015 [15]. Array hybridization and sample labeling were processed according to the manufacturer's protocol.

Using GeneSpring software V13.0 (Agilent), the circRNA array data summarization, normalization and quality control were obtained. The data were all Log2-transformed and median-centered by genes using the Adjust Data function of CLUSTER 3.0 software (Stanford University, Stanford, CA, USA), and further analyzed by applying hierarchical clustering with average linkage. Threshold values of ≥ 2 and ≤ − 2-fold change and a t test p value of 0.05 was regarded as proper for selecting the differentially expressed genes. Using Java Treeview (Stanford University School of Medicine, Stanford, CA, USA), we also performed tree visualization. The microarray data were analyzed with the help of CapitalBio Corporation (Beijing, People's Republic of China). Detailed clinical characteristics of the 12 patients in the microarray pilot group can be found in the supplementary data.

Quantitative real-time PCR (qRT-PCR)

Given the unique covalently closed loop structure of circRNAs, divergent primers rather than canonical convergent primers were designed through Primer-BLAST (NCBI, USA) to target the back-splicing sites, thus distinguishing circRNAs from their linear counterparts. Sequences of all circRNAs are available in certain sources (Circbase, Deepbase or Rybak-Wolf2015). Primers were synthesized by Sangon Biotech (Shanghai, China), and β-actin was chosen as the endogenous control. qRT-PCR was performed using the QuantiNova SYBR Green PCR Kit (QIAGEN GmbH, Hilden, Germany) and monitored with the StepOnePlus Real-Time PCR System (Applied Biosystems, Life Technologies, Waltham, MA, USA). The reactions were initiated in a 96-well optical plate at 95 °C for 2 min, followed by 40 cycles of 95 °C for 5 s and 60 °C for 10 s; each reaction was run in triplicate. The Ct values were determined with the fixed default settings (threshold 0.2, baseline start cycle: 3, end cycle: 15).

Statistical analysis

Data in this study were represented as the mean ± SD for quantitative variables. The Gaussian distribution of the continuous variables was tested by the Kolmogorov–Smirnov statistic. Student's t test for quantitative data with a Gaussian distribution or Mann–Whitney U test for quantitative data with a non-Gaussian distribution were used to evaluate the differences between groups. Cytoscape (version 3.2.1) was used to visualize the predictive network of circRNA/miRNA/mRNA. Statistical analysis was performed with GraphPad Version 6 (GraphPad Software Inc., San Diego, CA, USA). A p value < 0.05 was considered to be statistically significant. The relative expression level of each circRNA was presented using the $2^{-\Delta\Delta Ct}$ method.

Results

Expression profiles of circRNAs in CCs of PCOS patients

Hierarchical clustering and volcano plot revealed significant circRNA expression differences between two groups (Fig. 1); in total, 286 circRNAs were identified, including 167 that were upregulated and 119 that were downregulated in the PCOS group. To test the genuineness of the differentially expressed circRNAs revealed by microarray and to seek a potential novel biomarker for PCOS, we further validated six candidates (details are shown in Table 2) selected using a stricter screening criteria: fold change > 3.0, $p < 0.02$ and their relative raw intensity.

Gene ontology (GO) enrichment and KEGG pathway findings

Investigations of circRNA biogenesis have shown that circRNA and its linear isoform originate from the same pre-mRNA but are derived following different subsequent processing patterns [16]. The circulation of a given exon is mainly promoted by the flanking intronic sequences and back splicing, while canonical splicing contributes to

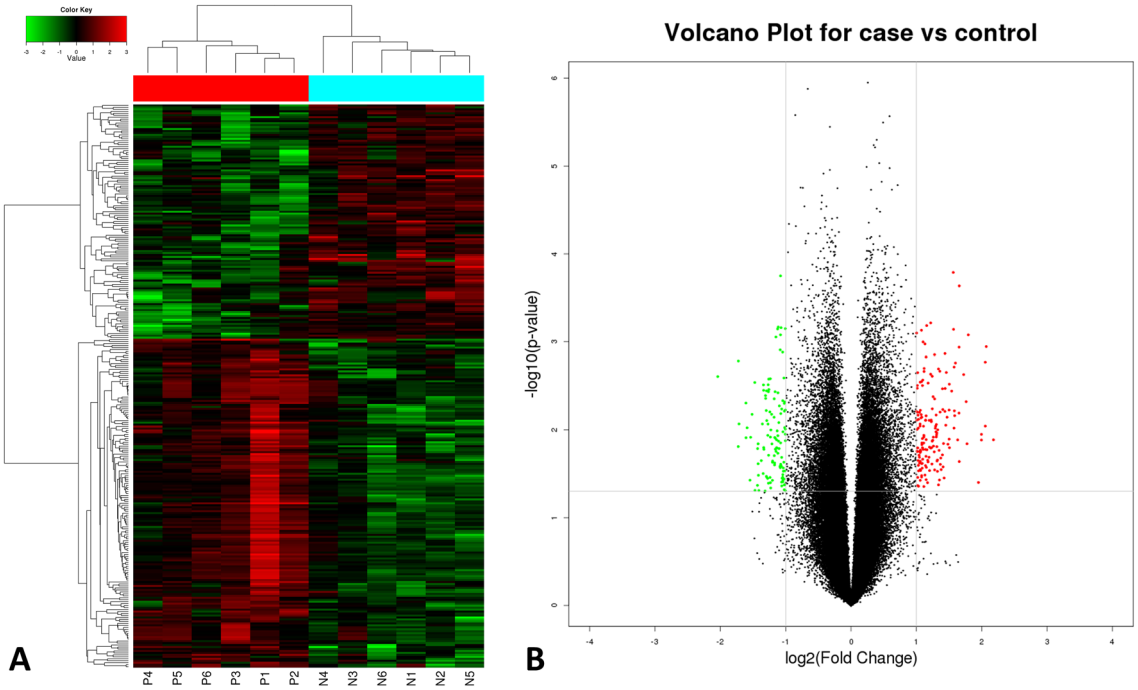

Fig. 1 Microarray results. **a** Cluster map of the circRNA microarray profiles in PCOS patients and control individuals. The expression of circRNAs is hierarchically clustered on the *y*-axis, numbers marked P and N on the *x*-axis represent different CC samples from PCOS patients and normal control individuals. **b** A volcano plot was constructed using fold-change values and *p* values. The vertical lines correspond to 2.0-fold up- and downregulation between CC samples from PCOS patients and normal control individuals, and the horizontal line represents a *p* value of 0.05. Red and green signs in the two figures represent statistically significant up- and downregulated circRNA expression in the PCOS group, respectively

Table 2 Profiles of six candidate circRNAs revealed by microarray

CircRNA	Regulation	Gene symbol	Fold change	*p* value	Source	Chr	Strand	Start	Stop
hsa_circ_0118530	Up	SF3B1	4.529029	0.012984	Rybak-Wolf2015	chr2	–	198,268,308	198,283,312
hsa_circ_0020491	Up	MKI67	4.198367	0.001135	Circbase	chr10	–	129,921,144	129,921,433
hsa_circ_0043533	Up	TOP2A	4.153623	0.009063	Circbase	chr17	–	38,544,772	38,556,319
hsa_circ_0097636	Down	KNTC1	4.113090	0.002476	Rybak-Wolf2015	chr12	+	123,028,705	123,047,246
hsa_circ_0043532	Up	TOP2A	3.421536	0.014409	Circbase	chr17	–	38,544,772	38,552,717
hsa_circ_0074576	Up	GPX3	3.1513854	0.000231	Circbase	chr5	+	150,406,992	150,408,554

the formation of its linear counterpart. General splicing factors are supposed to determine the balance between circRNA biogenesis and canonical splicing [16]. Further, circRNAs were reported to have potential regulatory effects on the expression of parental genes [17, 18]. Given the intricate relationship among circRNAs, their host gene and pre-mRNAs, GO enrichment and KEGG Pathway analysis (Fig. 2) were conducted in our study to better elucidate the novel role of dysregulated circRNAs in the pathogenesis of PCOS. We found that the most significantly enriched GO term in the biological process was organelle fission (GO: 0048285, $p = 1.978e-14$) (Fig. 2a); the most significantly enriched GO term in the cellular component was condensed chromosome outer kinetochore (GO: 0000940, $p = 4.798e-09$) (Fig. 2b); and the most significantly enriched GO term in the molecular function was cytoskeletal protein binding (GO: 0008092, $p = 1.140e-06$) (Fig. 2c). Among the top ten most significantly enriched KEGG pathways (Fig. 2d), cell cycle (hsa04110), oocyte meiosis (hsa04114) and progesterone-mediated oocyte maturation (hsa04914) are known to be involved in oocyte development. Furthermore, it had been reported that excess intraovarian androgen in PCOS might promote hyperfolliculogenesis mainly via the Foxo (hsa04068) and phosphatidylinositol signaling pathway (hsa04070) [19]. Finally, abnormal glycerophospholipid metabolism (hsa00564) has been shown to play a profound role in the pathogenesis of PCOS and complications of insulin resistance [20].

qRT-PCR validation

Three pairs of primers were designed for each circRNA, but only one resulted in a single peak (Fig. 3) in the melting curve used (Table 3). The results are shown in Fig. 4; the expression levels of hsa_circ_0043533 ($p < 0.01$) and hsa_circ_0074576 ($p < 0.05$) were significantly higher in the PCOS group while the expression level of hsa_circ_0097636 ($p < 0.01$) was significantly lower versus the non-PCOS group, which was consistent with the microarray data. Finally, hsa_circ_0118530, hsa_circ_0020491, and hsa_circ_0043532 showed no significant differences between the two groups.

Diagnostic value of novel circRNAs in PCOS

A receiver operating characteristic (ROC) curve was performed to determine the value of three novel circRNAs in distinguishing PCOS patients from normal control individuals (Fig. 5). The area under the ROC curve (AUC) of hsa_circ_0043533 was 0.709 (95% CI 0.566–0.851), and the sensitivity and specificity were 60 and 72%, respectively. Similarly, the AUC of hsa_circ_0043532 was 0.718 (95% CI 0.573–0.864), and the sensitivity and specificity were 56 and 88%, respectively. The AUC of hsa_circ_0097636 was 0.738 (95% CI 0.599–0.877), and the sensitivity and specificity were 52 and 96%, respectively. Intriguingly, when the serum testosterone (T) level was applied in combination with hsa_circ_0097636 using binary logistic regression analysis, the AUC increased significantly to 0.893 (95% CI 0.807–0.978), with 68% sensitivity and 100% specificity.

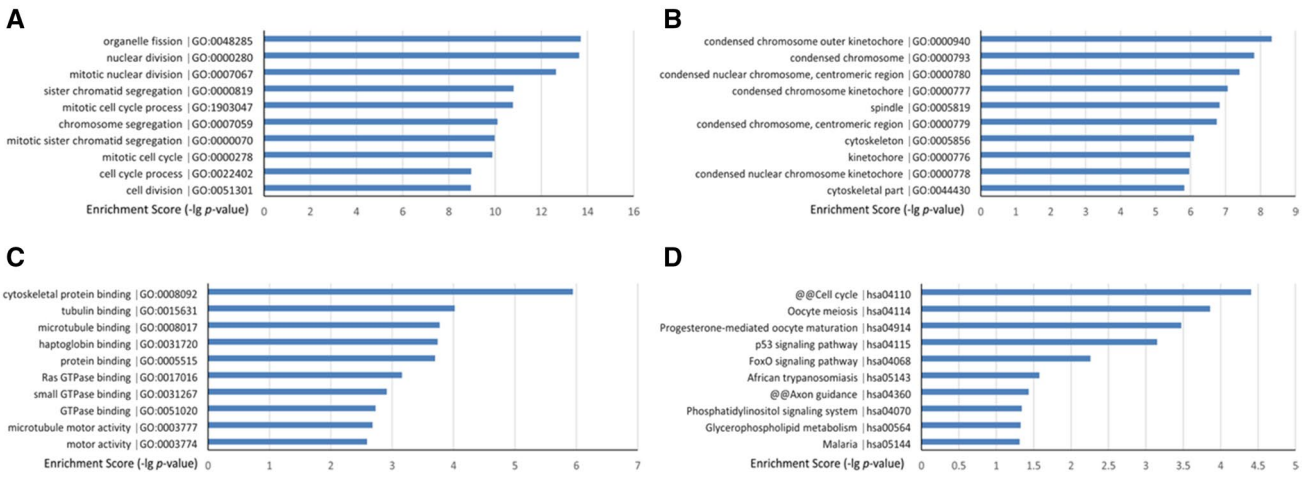

Fig. 2 GO enrichment and KEGG pathway analysis of dysregulated circRNAs gene symbols revealed by microarray. **a** Most significantly enriched GO (-lg *p* value) terms according to biological process. **b** Most significantly enriched GO (-lg *p* value) terms according to cellular component. **c** Most significantly enriched GO (-lg *p* value) terms according to molecular function. **d** Top ten significantly enriched KEGG pathways according to dysregulated circRNA gene symbols

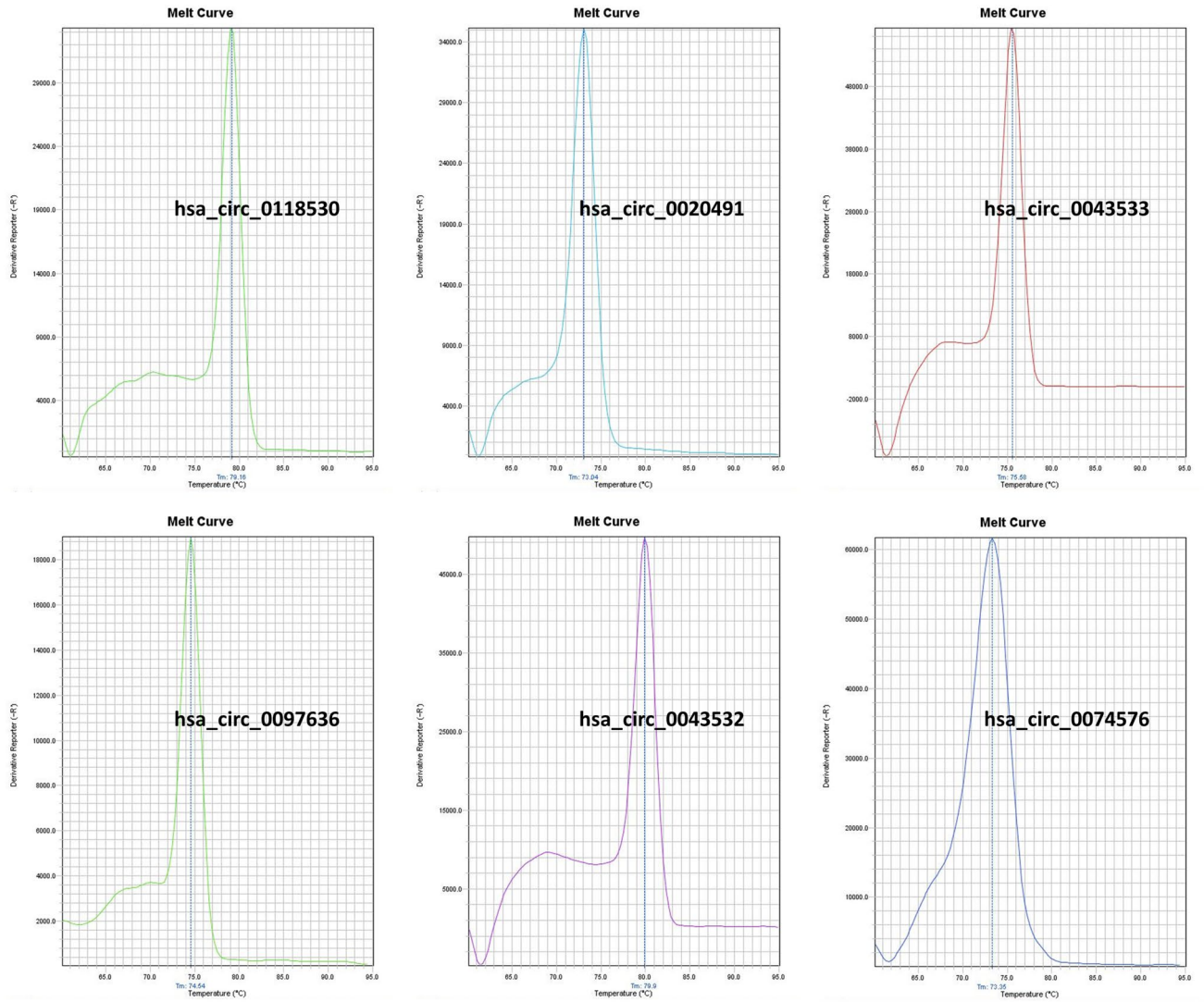

Fig. 3 Melt curves of six candidate circRNAs' qRT-PCR results, which all showed a single peak

Table 3 Paired primer sequences for the internal control and candidate circRNAs

	5′–3′	3′–5′
β-Actin	CTGGACTTCGAGCAAGAGATG	GAGTTGAAGGTAGTTTCGTGGA
hsa_circ_0118530	CCATATGTGCATAAGGAGGGAA	TGCTGCTCCATTGACGACTT
hsa_circ_0020491	ATGAGCCTGTACGGCTAAAACA	CATTCAATACCCCTGAAGGAACG
hsa_circ_0043533	AACCCAGTGCTTTTTGACCAC	CCAAGCATTCCTAGGAGCCAT
hsa_circ_0097636	CCAGAAAAATTCAGTTACAAGGACA	TCCAGCCACAAGACTGAGAC
hsa_circ_0043532	ATTGCAACCCAGCTGTTGAAGC	AGGCAAAACTTCAGCCATTTGT
hsa_circ_0074576	TGCAGCAGCTGAGTATGTCC	ATCCCCTTTCTCAAAGAGCTGG

Prediction and annotation of the ceRNA network using the three validated circRNAs potentially involved in PCOS

To investigate the biological role of the three validated circRNAs, we used bioinformatic tools to predict their potential targets and visualize the interactive network (Fig. 6). The most important and widely recognized function of circRNAs is acting as an miRNA sponge; therefore, we first manually selected all miRNAs which have been reported to have a role in the pathogenesis of PCOS and then tested whether they have potential binding sites for the three dysregulated

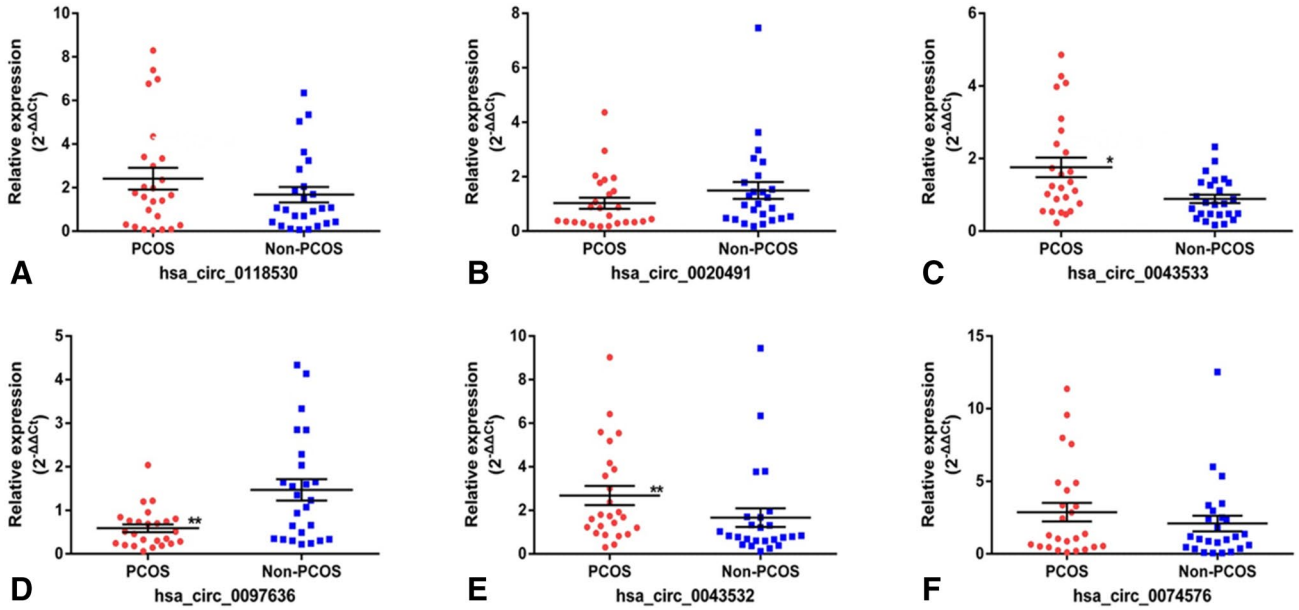

Fig. 4 Relative expression levels of six candidate circRNAs quantified by qRT-PCR between the PCOS ($n=25$) and non-PCOS ($n=25$) groups. The expression levels of hsa_circ_0043533 (**c**, $*p<0.05$) and hsa_circ_0043532 (**e**, $**p<0.01$) were significantly higher in the PCOS group, and the expression level of hsa_circ_0097636 (**d**, $**p<0.01$) was significantly lower versus the non-PCOS group. hsa_circ_0118530 (**a**, $p=0.4157$), hsa_circ_0020491 (**b**, $p=0.1536$) and hsa_circ_0074576 (**f**, $p=0.4440$) showed no significant differences between the two groups

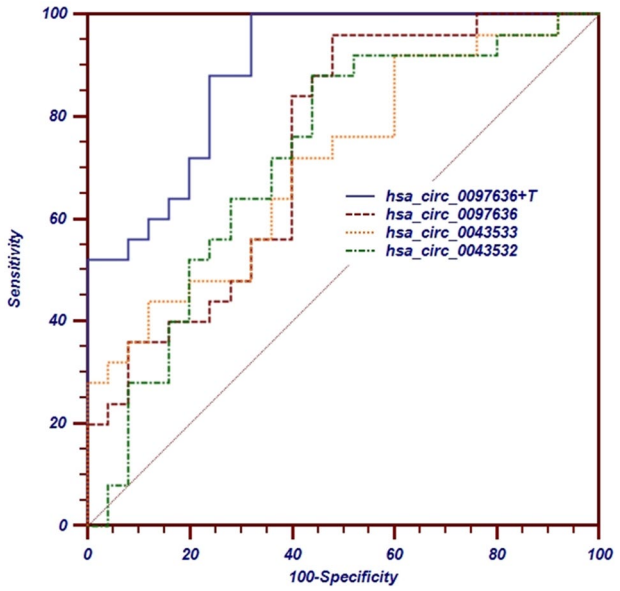

Fig. 5 ROC curves revealed that serum testosterone (T) level combined with hsa_circ_0097636 enhanced the efficacy of distinguishing PCOS patients from normal control individuals. The AUC of hsa_circ_0097636, hsa_circ_0043533, and hsa_circ_0043532 alone was 0.738 (95% CI 0.599–0.877), 0.709 (95% CI 0.566–0.851), and 0.718 (95% CI 0.573–0.864), respectively. The AUC of combination model (hsa_circ_0097636 + T) increased significantly to 0.893 (95% CI 0.807–0.978)

circRNAs by miRanda (34.236.212.39/microrna/home.do) and TargetScan (http://www.targetscan.org/vert_71/). We also predicted miRNA potential binding with the input genes involved in the six significantly enriched KEGG pathways related to PCOS. Remarkably, the coprediction revealed that four input genes (FOXO3, DGKI, PCYT1B, and CCNB1) have binding sites for the three validated circRNAs' potential target miRNAs.

Discussion

PCOS is widely considered an intricate trait resulting from the intrinsic interaction of multiple inherited and environmental factors that first manifests at adolescence on most occasions [21]. To date, many signaling cascades have been proposed in the pathogenesis of PCOS and hold great promise as potential targets for effective treatment strategies, including the MAPK-ERK [14], Wnt/β-catenin [22] and PI3 K-Akt [23] pathways. Although the exact etiology of PCOS remains obscure, its clinical manifestations are also highly heterogeneous, including abnormal folliculogenesis, aberrant steroidogenesis, prominent functional ovarian hyperandrogenism, and adipocyte dysfunction are the major features.

Although the first evidence was in the early 1970s in higher plants, the history of circRNA research is relatively short due to the lack of useful techniques and tools. Only

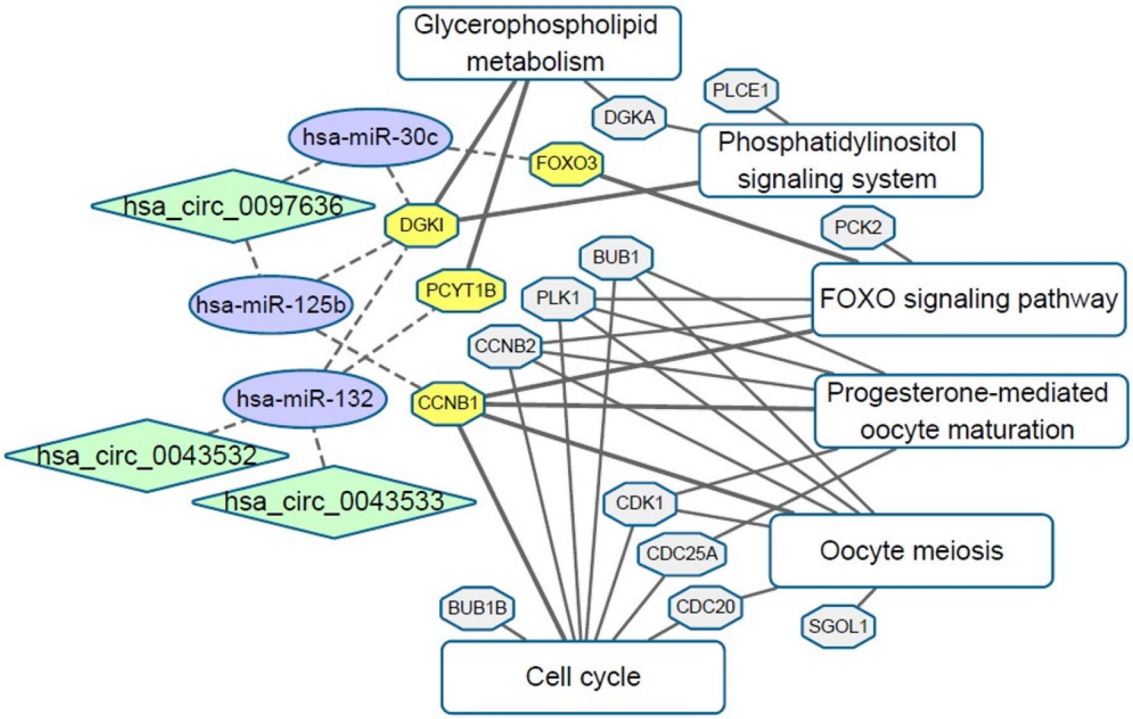

Fig. 6 Mapping of the predictive interaction network of circRNA/miRNA/mRNA and six significantly enriched KEGG pathways related to PCOS. White rectangles represent KEGG pathways and octagons indicate input genes involved in the pathways: those in yellow are predicted to have binding sites for miRNAs by TargetScan

when RNA deep-sequencing technology and bioinformatics became highly developed over the past decade did scientists realize that circRNAs are far more than simple byproducts from mis-splicing during transcription but are rather a sort of ubiquitous, conserved, abundant and stable type of RNA molecule with great regulatory potency [5]. Until now, several roles for circRNAs at the transcriptional and post-transcriptional level have been proposed and investigated [24]. The most cardinal and well-studied function is as an miRNA sponge—a human circRNA, antisense to the cerebellar degeneration-related protein 1 transcript (CDR1as), was found to harbor 63 miR-7 in neuronal tissues. Similar to knocking down miR-7, midbrain development in zebrafish was impaired by the expression of human CDR1as [25]. In most studies, the expression of a certain circRNA normally downregulates its target miRNA and subsequently improves the expression of specific mRNAs and proteins downstream. For instance, upregulated circHIPK3 in diabetic retinas increased the expression of VEGF-C, FZD4 and WNT2 by sequestering the activity of miR-30a-3p through a "sponge mechanism", which led to endothelial proliferation and vascular dysfunction [9]. A heart-related circRNA termed HRCR by Wang et al. was reported to act as an endogenous miR-223 sponge, which negatively regulated miR-223 function in cardiac hypertrophy [26]. Strikingly, a novel and opposing effect of circRNA was recently delineated [27] when *Cdr1as*-knockout animals displayed a prominent neuropsychiatric phenotype with destabilized mature miR-7 and enhanced expression of *Fos* and *Nr4a3* in neurons, direct targets of miR-7. These findings may suggest more intricate and profound functions of circRNAs in the competing endogenous RNA (ceRNA) networks, which still requires in-depth investigation.

Compared to circRNAs, studies on miRNAs have been relatively well established. Studies to date have unveiled numerous miRNAs with significant regulatory effects in circulating blood, follicular fluid and granulosa cells of patients with PCOS. For example, miR-93 is upregulated in the adipose tissue of PCOS patients, and can downregulate the expression of insulin-sensitive glucose transporter isoform 4 (GLUT-4) through direct targeting of the 3′ UTR of GLUT-4, leading to insulin resistance [28]. miR-145 suppresses the proliferation of isolated granulosa cells from PCOS patients by targeting insulin receptor substrate 1 (IRS1) and subsequently inhibiting the MAPK/ERK signaling pathway [29]. miR-320a was found to be significantly downregulated in CCs from patients with PCOS, which impaired its modulation of CYP11A1 and CYP19A1 in the process of steroidogenesis thus contributing to the development of estrogen deficiency in CCs [30].

In light of the unique property of circRNAs as "miRNA sponges" corroborated by previous studies, we first detected

the expression of novel circRNAs in the CCs of patients with PCOS, and three (hsa_circ_0043533, hsa_circ_0097636, and hsa_circ_0043532) of six were found to be dysregulated through qRT-PCR. Spearman's rank correlation (Table 4) indicated that the serum T level positively correlated with both the expression of hsa_circ_0043533 and hsa_circ_0097636 in the PCOS group. It has been commonly acknowledged that most PCOS is due to hyperandrogenism arising from dysregulation of steroidogenesis in theca cells that are oversensitive to LH, while a previous study [31] found that female androgen-receptor knockout mice had crucial reproductive defects, indicating androgen's vital role in the balance between follicle growth and follicular atresia. In this study, we also predicted circRNA–miRNA interactions (Fig. 6) by miRanda and TargetScan. Among the numerous potential targeting miRNAs, surprisingly, we found that miR-125b and miR-30c had potential binding sites for hsa_circ_0097636, miR-132 for hsa_circ_0043533, and hsa_circ_0043532. All of these predicted miRNAs have been previously studied in PCOS [31–34]. miRNA-125b has been reported to be an anti-apoptotic miRNA and one of the most plentiful miRNAs in the ovary among different species [35]. It can be upregulated by excess androgen and subsequently prevent the ovarian follicle from apoptosis and atresia [31], which may also explain the hyperfolliculogenesis in PCOS patients with hyperandrogenemia. miR-30c was observed to be upregulated in the serum of PCOS patients and rat granulosa cells following FSH exposure [32, 36]. The upregulated expression of miRNA-125b and miR-30c described in previous studies and the downregulation of has_circ_0097636 validated in our work may together be involved in the onset of PCOS. Likewise, through genome-scale screening, miR-132 was identified to inhibit the release of all three steroid hormones (P, E_2 and T) in human ovarian cells [34]. Hence, we speculate that upregulated hsa_circ_0043533 and hsa_circ_0043532 likely play a significant role in altering steroidogenesis in PCOS by targeting miRNA-132, but further studies are warranted to explore whether our speculation is true and to reveal the exact underlying mechanisms. To summarize, these three dysregulated circRNAs may have potential significance in the abnormal hyperfolliculogenesis and steroidogenesis in PCOS patients by targeting circRNA–miRNA interactions.

Additionally, ROC curves revealed that a combination model using the serum T level and hsa_circ_0097636 significantly enhanced the efficacy of distinguishing PCOS patients from normal control individuals; the AUC was 0.893 (95% CI 0.807–0.978) with 68% sensitivity and 100% specificity. In a previous study, many miRNAs including miR-146a, miR-93 and let-7b were proposed as valuable biomarkers for PCOS [32, 37, 38]. Considering its high cytoplasmic stability, we speculate that using a certain circRNA, such as hsa_circ_0097636, together with the serum T level as the screening criteria could be of great diagnostic value for PCOS.

To the best of our knowledge, this study is the first to detect novel circRNA expression in the cumulus cells of patients with PCOS. We validated several dysregulated

Table 4 Spearman's rank correlation coefficients of the expression of three differentially expressed circRNAs and paticipants' partial clinical characteristics

	PCOS group		Non-PCOS group	
	r	*p* value	*r*	*p* value
hsa_circ_0043533				
Age	−0.1320	0.5294	0.1486	0.4882
BMI	0.0881	0.6752	−0.0936	0.6637
LH	−0.0573	0.7855	0.1652	0.4404
FSH	0.0281	0.8940	−0.1670	0.4355
LH/FSH	−0.1381	0.5103	0.1705	0.4257
E_2	−0.0700	0.7395	−0.0904	0.7153
T	0.3999	**0.0476**	−0.3779	0.0686
P	0.3593	0.5294	0.1486	0.4882
Oocytes obtained	0.0844	0.688	40.1812	0.3967
HQ embryos	−0.0788	0.7083	0.3799	0.0671
Rate of HQ embryos	−0.1418	0.4988	0.3990	0.0534
hsa_circ_0097636				
Age	−0.1545	0.4609	−0.1738	0.4767
BMI	−0.1105	0.5991	−0.2563	0.2896
LH	0.2677	0.1957	0.0684	0.7808
FSH	0.0823	0.6956	0.1509	0.5375
LH/FSH	0.2777	0.1789	−0.0746	0.7614
E_2	0.2954	0.1517	0.6088	**0.0057**
T	0.5075	**0.0096**	−0.2321	0.3389
P	0.1986	0.3413	0.2140	0.3789
Oocytes obtained	0.1653	0.4297	−0.3176	0.1990
HQ embryos	0.1173	0.5766	−0.3898	0.1098
Rate of HQ embryos	0.1393	0.5066	−0.3536	0.1501
hsa_circ_0043532				
Age	0.0125	0.9550	−0.1436	0.5346
BMI	0.1790	0.4138	−0.7371	**0.0001**
LH	−0.0983	0.6553	−0.0935	0.6868
FSH	0.0776	0.7249	0.2455	0.2835
LH/FSH	−0.1003	0.6488	−0.2730	0.2312
E_2	−0.1265	0.5652	0.2273	0.3218
T	0.1172	0.5943	−0.3005	0.1856
P	−0.1033	0.5943	−0.0013	0.9955
Oocytes obtained	−0.2249	0.3023	−0.1736	0.4518
HQ embryos	−0.1835	0.4019	0.3040	0.1803
Rate of HQ embryos	0.0842	0.7026	0.2477	0.2790

Spearman's rank correlation of coefficients was performed since the relative expression level of circRNAs did not conform to a Gaussian distribution

r correlation coefficient, $p < 0.05$ is in bold and considered to be statistically significant

circRNAs, which may offer great promise to better understanding the pathogenesis and to develop effective therapeutic interventions for PCOS patients. Due to the limited size of the samples in the present study, a larger population and the specific mechanisms underlying circRNA involvement are required for further investigation.

Acknowledgements This work was financially supported by the National Natural Science Foundation of China (No. 81671416).

Author contributions ZM: data collection, formal analysis, manuscript writing. HZ: methodology and software supporting. YZ: methodology supporting and manuscript editing. XL: sample collection. CH: project development and manuscript editing.

Compliance with ethical standards

Conflict of interest We declare no conflict of interest.

Ethical statement This study was approved by the Institutional Ethics Review Board, Yantai Yuhuangding Hospital affiliated to Qingdao University.

References

1. Yildiz BO, Bozdag G, Yapici Z et al (2012) Prevalence, phenotype and cardiometabolic risk of polycystic ovary syndrome under different diagnostic criteria. Hum Reprod 27:3067–3073
2. Broekmans FJ, Knauff EA, Valkenburg O et al (2006) PCOS according to the Rotterdam consensus criteria: change in prevalence among WHO-II anovulation and association with metabolic factors. BJOG 113:1210–1217
3. Diao FY, Xu M, Hu Y et al (2004) The molecular characteristics of polycystic ovary syndrome (PCOS) ovary defined by human ovary cDNA microarray. J Mol Endocrinol 33:59–72
4. Teede HJ, Misso ML, Deeks AA et al (2011) Assessment and management of polycystic ovary syndrome: summary of an evidence-based guideline. Med J Aust 195:S65–112
5. Salzman J (2016) Circular RNA expression: its potential regulation and function. Trends Genet 32:309–316
6. Qu S, Yang X, Li X et al (2015) Circular RNA: a new star of noncoding RNAs. Cancer Lett 365:141–148
7. Rybak-Wolf A, Stottmeister C, Glazar P et al (2015) Circular RNAs in the mammalian brain are highly abundant, conserved, and dynamically expressed. Mol Cell 58:870–885
8. Legnini I, Di Timoteo G, Rossi F et al (2017) Circ-ZNF609 is a circular RNA that can be translated and functions in myogenesis. Mol Cell 66:22–37.e29
9. Shan K, Liu C, Liu BH et al (2017) Circular noncoding RNA HIPK3 mediates retinal vascular dysfunction in diabetes mellitus. Circulation 136:1629–1642
10. Jeck WR, Sharpless NE (2014) Detecting and characterizing circular RNAs. Nat Biotechnol 32:453–461
11. Dang Y, Yan L, Hu B et al (2016) Tracing the expression of circular RNAs in human pre-implantation embryos. Genome Biol 17:130
12. Cheng J, Huang J, Yuan S et al (2017) Circular RNA expression profiling of human granulosa cells during maternal aging reveals novel transcripts associated with assisted reproductive technology outcomes. PLoS One 12:e0177888
13. Rotterdam EA-SPCWG (2004) Revised 2003 consensus on diagnostic criteria and long-term health risks related to polycystic ovary syndrome. Fertil Steril 81:19–25
14. Huang X, Liu C, Hao C et al (2016) Identification of altered microRNAs and mRNAs in the cumulus cells of PCOS patients: miRNA-509-3p promotes oestradiol secretion by targeting MAP3 K8. Reproduction 151:643–655
15. You X, Vlatkovic I, Babic A et al (2015) Neural circular RNAs are derived from synaptic genes and regulated by development and plasticity. Nat Neurosci 18:603–610
16. Ashwal-Fluss R, Meyer M, Pamudurti NR et al (2014) circRNA biogenesis competes with pre-mRNA splicing. Mol Cell 56:55–66
17. Zhang Y, Zhang XO, Chen T et al (2013) Circular intronic long noncoding RNAs. Mol Cell 51:792–806
18. Li Z, Huang C, Bao C et al (2015) Exon-intron circular RNAs regulate transcription in the nucleus. Nat Struct Mol Biol 22:256–264
19. Yang JL, Zhang CP, Li L et al (2010) Testosterone induces redistribution of forkhead box-3a and down-regulation of growth and differentiation factor 9 messenger ribonucleic acid expression at early stage of mouse folliculogenesis. Endocrinology 151:774–782
20. Chen YX, Zhang XJ, Huang J et al (2016) UHPLC/Q-TOFMS-based plasma metabolomics of polycystic ovary syndrome patients with and without insulin resistance. J Pharm Biomed Anal 121:141–150
21. Rosenfield RL, Ehrmann DA (2016) The pathogenesis of polycystic ovary syndrome (PCOS): the hypothesis of PCOS as functional ovarian hyperandrogenism revisited. Endocr Rev 37:467–520
22. Chazenbalk G, Chen YH, Heneidi S et al (2012) Abnormal expression of genes involved in inflammation, lipid metabolism, and Wnt signaling in the adipose tissue of polycystic ovary syndrome. J Clin Endocrinol Metab 97:E765–770
23. Zhao Y, Zhang C, Huang Y et al (2015) Up-regulated expression of WNT5a increases inflammation and oxidative stress via PI3K/AKT/NF-kappaB signaling in the granulosa cells of PCOS patients. J Clin Endocrinol Metab 100:201–211
24. Barrett SP, Salzman J (2016) Circular RNAs: analysis, expression and potential functions. Development 143:1838–1847
25. Memczak S, Jens M, Elefsinioti A et al (2013) Circular RNAs are a large class of animal RNAs with regulatory potency. Nature 495:333–338
26. Wang K, Long B, Liu F et al (2016) A circular RNA protects the heart from pathological hypertrophy and heart failure by targeting miR-223. Eur Heart J 37:2602–2611
27. Piwecka M, Glazar P, Hernandez-Miranda LR et al (2017) Loss of a mammalian circular RNA locus causes miRNA deregulation and affects brain function. Science 357:6357
28. Chen YH, Heneidi S, Lee JM et al (2013) miRNA-93 inhibits GLUT4 and is overexpressed in adipose tissue of polycystic ovary syndrome patients and women with insulin resistance. Diabetes 62:2278–2286
29. Cai G, Ma X, Chen B et al (2017) MicroRNA-145 negatively regulates cell proliferation through targeting IRS1 in isolated ovarian granulosa cells from patients with polycystic ovary syndrome. Cell Biochem Funct 24:902–910
30. Zhang CL, Wang H, Yan CY et al (2017) Deregulation of RUNX2 by miR-320a deficiency impairs steroidogenesis in cumulus granulosa cells from polycystic ovary syndrome (PCOS) patients. Biochem Biophys Res Commun 482:1469–1476
31. Sen A, Prizant H, Light A et al (2014) Androgens regulate ovarian follicular development by increasing follicle stimulating hormone receptor and microRNA-125b expression. Proc Natl Acad Sci USA 111:3008–3013
32. Long W, Zhao C, Ji C et al (2014) Characterization of serum microRNAs profile of PCOS and identification of novel non-invasive biomarkers. Cell Physiol Biochem 33:1304–1315

33. Sang Q, Yao Z, Wang H et al (2013) Identification of microRNAs in human follicular fluid: characterization of microRNAs that govern steroidogenesis in vitro and are associated with polycystic ovary syndrome in vivo. J Clin Endocrinol Metab 98:3068–3079
34. Sirotkin AV, Ovcharenko D, Grossmann R et al (2009) Identification of microRNAs controlling human ovarian cell steroidogenesis via a genome-scale screen. J Cell Physiol 219:415–420
35. Donadeu FX, Schauer SN, Sontakke SD (2012) Involvement of miRNAs in ovarian follicular and luteal development. J Endocrinol 215:323–334
36. Yao N, Yang BQ, Liu Y et al (2010) Follicle-stimulating hormone regulation of microRNA expression on progesterone production in cultured rat granulosa cells. Endocrine 38:158–166
37. Sathyapalan T, David R, Gooderham NJ et al (2015) Increased expression of circulating miRNA 93 in women with polycystic ovary syndrome may represent a novel, non-invasive biomarker for diagnosis. Sci Rep 5:16890
38. Scalici E, Traver S, Mullet T et al (2016) Circulating microRNAs in follicular fluid, powerful tools to explore in vitro fertilization process. Sci Rep 6(24976):3